PERGAMON

International Journal of Solids and Structures 40 (2003) 573–590

INTERNATIONAL JOURNAL OF SOLIDS and STRUCTURES

www.elsevier.com/locate/ijsolstr

Penny shaped crack in a piezoelectric cylinder surrounded by an elastic medium subjected to combined in-plane mechanical and electrical loads

Ji Hyuck Yang *, Kang Yong Lee *

Department of Mechanical Engineering, Graduate School, Yonsei University, Seoul 120-749, South Korea

Received 29 April 2002; received in revised form 9 October 2002

Abstract

The fracture problem of a penny shaped crack in a piezoelectric ceramic cylinder surrounded by an infinite elastic medium under in-plane normal mechanical and electrical loads is considered with the electric continuous boundary conditions on the crack surface. By using the potential theory and Hankel transform, a system of dual integral equations is obtained, and expressed to a Fredholm integral equation of the second kind. The mechanical and electrical field equations and all sorts of field intensity factors of mode I are obtained, and the numerical values of various field intensity factors for PZT-6B piezoelectric ceramic surrounded by several different elastic media are graphically shown for a uniform load and a ring-shaped load, respectively. And the effects of the size of the piezoelectric cylinder and the elastic material properties on various field intensity factors are obtained.

Keywords: Piezoelectric cylinder; Mode I; Penny shaped crack; Elastic medium; Stress intensity factor; Field intensity factor; Fredholm integral equation

1. Introduction

Since piezoelectric ceramics which are typical brittle materials usually contain micro defects during the sintering process, the equipments of piezoelectric ceramics have the risk of the abrupt fracture or the functional disorder. Therefore, their fracture behaviors due to the micro defects under mechanical and electrical loads have become great interest and a lot of significant researches have been presented recently. Pak (1990) obtained the closed form solutions of field intensity factors and the energy release rate for an infinite piezoelectric medium under anti-plane load by using a complex variable method. Park and Sun (1995a) obtained the closed form solutions of the stress intensity factor, the total energy release rate and the mechanical strain energy release rate for all three modes of fracture for an infinite piezoelectric medium with insulated crack surfaces subjected to a combined mechanical and electrical loads by using Stroh formalism approach. Shindo et al. (1997) obtained the solutions of the stress intensity factor and the energy

* Corresponding authors. Fax: +82-2-2123-2813.
E-mail addresses: sunnyspot@orgio.net (J.H. Yang), kyl2813@yahoo.co.kr (K.Y. Lee).

0020-7683/02/$ - see front matter © 2002 Published by Elsevier Science Ltd.
PII: S0020-7683(02)00620-0

release rate for the infinite strip perpendicular to the line crack under anti-plane load by using integral transform method.

For the electric boundary conditions on the crack surfaces of a piezoelectric medium, several conditions have been brought up and none explains the real phenomenon exactly. The impermeable electric boundary condition on the crack surface has been widely used in the previous works (Pak, 1990; Park and Sun, 1995a; Sosa, 1991). However, as pointed out by Dunn (1994), Sosa and Khutoryansky (1996), Zhang and Tong (1996), Gao and Fan (1999a), Chen and Shioya (1999) and Shindo et al. (2001), the results under impermeable conditions show a non-physical singularity around the crack and disagree with experimental results. For example, the total energy release rate in case of the impermeable boundary condition under an electrical load only is always negative. Jackson (1976) suggested that the normal components of the electric displacement and the tangential components of the electric field should be continuous across the crack surface because real cracks in piezoelectric media are filled with vacuum or air. McMeeking (1989), Zhang and Hack (1992), Zhang and Tong (1996) and Gao and Fan (1999b) adopted this electrical condition and their results are reasonable.

The crack problems for the piezoelectric ceramics have been usually concentrated to simple line cracks. But three-dimensional crack, such as a penny-shaped crack and an elliptical crack, exists in real media frequently. Wang (1992) obtained the field intensity factors for an elliptical crack in infinite piezoelectric media by using Fourier transform method with the electric impermeable condition. Wang and Huang (1995) and Wang and Zheng (1995) showed the general solutions of the field intensity factors expressed by potential functions for an elliptical crack of a three-dimensional piezoelectric medium under the electric impermeable condition. Kogan and Hui (1996) showed the closed form solutions of the field intensity factors for a spheroidal piezoelectric inclusion in an infinite piezoelectric medium by using potential theory, and presented the results for a penny shaped crack as a limiting case of the original problem. Zhao et al. (1997a,b) obtained the fundamental solutions for a unit concentrated displacement and an electric potential discontinuity in a three-dimensional piezoelectric medium, and the stress intensity factor for a circular crack in a piezoelectric solid. Recently, Chen and Shioya (2000) obtained the modes II and III stress intensity factors of a penny shaped crack under arbitrary shear load by using Fabrikant's elastic results (Fabrikant, 1989). But all previous works were studied for the unbounded media and most of them treated the uniform loads. Recently, the three-dimensional crack problem in a piezoelectric strip with finite thickness under axisymmetric loads was investigated by us (Yang and Lee, 2001).

In this paper, we consider the penny shaped crack in a three-dimensional piezoelectric ceramic cylinder surrounded by an elastic medium under both in-plane mechanical and electrical loads. The electric continuous boundary condition on the crack surfaces is adopted. The potential theory and Hankel transform method are used to obtain a system of dual integral equations, which is then expressed to a Fredholm integral equation of the second kind. The general forms and numerical results for various field intensity factors are given for PZT-6B piezoelectric ceramics surrounded by several different elastic media for a uniform load and a ring-shaped load, respectively. Consequently, the effects of the ratio of crack radius to cylinder radius, the mechanical and electrical loads and the kind of elastic material on the crack propagation are shown.

2. Problem statements

Consider a piezoelectric ceramic cylinder of diameter $2b$ surrounded by an elastic medium containing a center penny-shaped crack of diameter $2a$ which is perpendicular to the side surface under the mechanical and electrical normal loads as shown in Fig. 1. The superscripts (p) and (e) mean the piezoelectric and elastic medium, respectively. The system of cylindrical coordinates (r, θ, z) is set at the center of the crack. The piezoelectric ceramic is transversely isotropic with hexagonal symmetry and the z-axis is oriented in the poling direction, and the elastic medium is also transversely isotropic. The ceramic is subjected to a normal

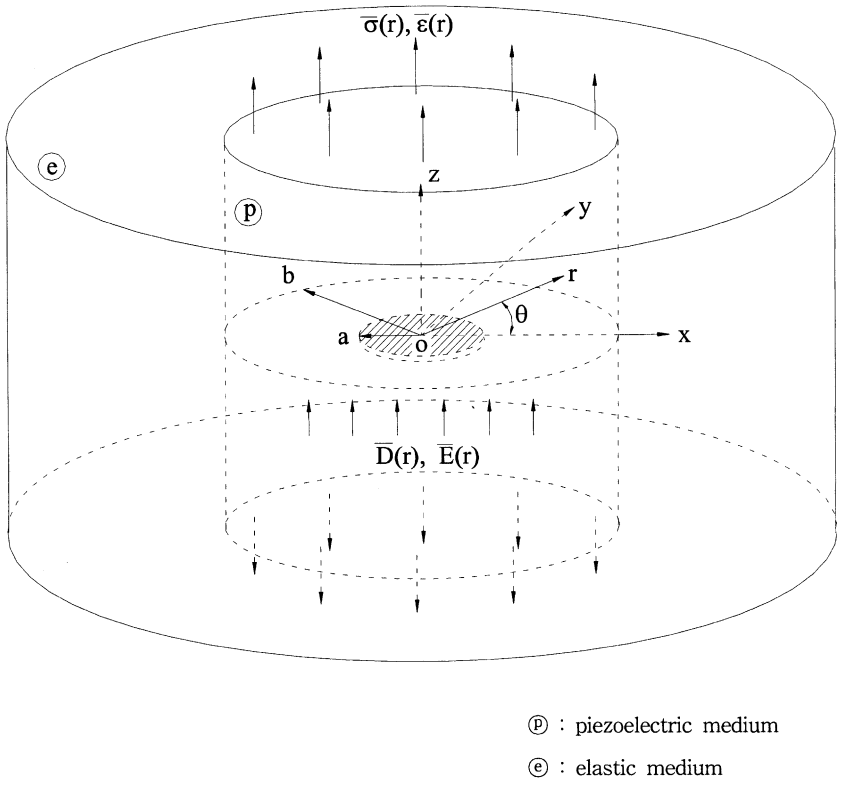

Fig. 1. Piezoelectric cylinder with a penny shaped crack surrounded by an infinite elastic medium under in-plane normal mechanical and electrical loads.

stress or strain at infinity, and the electrical loading condition of an electric displacement or electric field for the piezoelectric ceramic is considered (Pak, 1990; Yang and Lee, 2001).

In the absence of body forces, the equations of motion are,

$$\frac{\partial \sigma_r^{(j)}}{\partial r}+\frac{\partial \sigma_{rz}^{(j)}}{\partial z}+\frac{\sigma_r^{(j)}-\sigma_\theta^{(j)}}{r}=0, \qquad \frac{\partial \sigma_{rz}^{(j)}}{\partial r}+\frac{\partial \sigma_z^{(j)}}{\partial z}+\frac{\sigma_{rz}^{(j)}}{r}=0, \tag{1}$$

where $j=\mathrm{p},\mathrm{e}$, and the equation of electrostatics for the piezoelectric medium only is,

$$\frac{\partial D_r}{\partial r}+\frac{\partial D_z}{\partial z}+\frac{D_r}{r}=0, \tag{2}$$

where σ_k $(k=r,\theta,z)$ and σ_{rz} are normal and shear stresses, respectively and D_k $(k=r,z)$ are electric displacements.

In the piezoelectric medium, using the gradient equations and the constitutive equations, Eqs. (1) and (2) become governing equations. To get the solutions which satisfy the governing equations, we define the potentials in the forms,

$$u_r^{(\mathrm{p})}=\sum_{i=1}^{3}\frac{\partial \Phi_i}{\partial r}, \qquad u_z^{(\mathrm{p})}=\sum_{i=1}^{3}k_{1i}\frac{\partial \Phi_i}{\partial z}, \qquad \phi=-\sum_{i=1}^{3}k_{2i}\frac{\partial \Phi_i}{\partial z}, \tag{3}$$

where u_k $(k=r,z)$ are displacements, ϕ is electric potential, $\Phi_i(r,z)$ $(i=1,2,3)$ are the potential functions, k_{1i} and k_{2i} $(i=1,2,3)$ are unknown constants in the piezoelectric medium.

Using Eqs. (1)–(3), we can get the governing equation in the form,

$$\frac{\partial^2 \Phi_i}{\partial r^2} + \frac{1}{r}\frac{\partial \Phi_i}{\partial r} + \frac{\partial^2 \Phi_i}{\partial z_i^2} = 0 \quad (i = 1, 2, 3), \tag{4}$$

where

$$z_i = \frac{z}{\sqrt{n_i}} = s_i z \quad (i = 1, 2, 3), \tag{5}$$

and n_i $(i = 1, 2, 3)$ are obtained from the following equation:

$$An_i^3 + Bn_i^2 + Cn_i + D = 0, \tag{6}$$

where

$$\begin{aligned} A &= c_{44}d_{11} + e_{15}^2, \\ B &= \left(d_{11}c_{13}^2 - c_{11}c_{33}d_{11} + 2c_{13}c_{44}d_{11} - c_{11}c_{44}d_{33} + 2c_{13}e_{15}^2 + 2c_{13}e_{15}e_{31} - c_{44}e_{31}^2 - 2c_{11}e_{15}e_{33}\right)/c_{11}, \\ C &= \left(c_{33}c_{44}d_{11} - c_{13}^2 d_{33} + c_{11}c_{33}d_{33} - 2c_{13}c_{44}d_{33} + c_{33}e_{15}^2 + 2c_{33}e_{15}e_{31}\right. \\ &\quad \left. + c_{33}e_{31}^2 - 2c_{13}e_{15}e_{33} - 2c_{13}e_{31}e_{33} - 2c_{44}e_{31}e_{33} + c_{11}e_{33}^2\right)/c_{11}, \\ D &= -c_{44}\left(c_{33}d_{33} + e_{33}^2\right)/c_{11}, \end{aligned} \tag{7}$$

k_{1i} and k_{2i} $(i = 1, 2, 3)$ are determined from the following equations,

$$n_i = \frac{c_{44} + (c_{13} + c_{44})k_{1i} - (e_{31} + e_{51})k_{2i}}{c_{11}} = \frac{c_{33}k_{1i} - e_{33}k_{2i}}{c_{44}k_{1i} + c_{13} + c_{44} - e_{15}k_{2i}} = \frac{e_{33}k_{1i} + d_{33}k_{2i}}{e_{15}k_{1i} + e_{15} + e_{31} + d_{11}k_{2i}}, \tag{8}$$

where c_{11}, c_{12}, c_{13}, c_{33} and c_{44} are the elastic moduli measured in a constant electric field; d_{11} and d_{33} are the dielectric permittivities measured at a constant strain; and e_{15}, e_{31} and e_{33} are the piezoelectric constants in the piezoelectric material.

In the elastic medium, we define the potentials in the forms,

$$u_r^{(e)} = \sum_{i=1}^{2} \frac{\partial \widetilde{\Phi}_i}{\partial r}, \qquad u_z^{(e)} = \sum_{i=1}^{2} \tilde{k}_i \frac{\partial \widetilde{\Phi}_i}{\partial z}, \tag{9}$$

where $\widetilde{\Phi}_i(r, z)$ $(i = 1, 2)$ are the potential functions, and $\tilde{k}_i$ $(i = 1, 2)$ are unknown constants in the elastic medium. Using Eqs. (1), (9), gradient equations and the constitutive equations, we can get the governing equation in the elastic medium in the form,

$$\frac{\partial^2 \widetilde{\Phi}_i}{\partial r^2} + \frac{1}{r}\frac{\partial \widetilde{\Phi}_i}{\partial r} + \frac{\partial^2 \widetilde{\Phi}_i}{\partial \tilde{z}_i^2} = 0 \quad (i = 1, 2), \tag{10}$$

where

$$\tilde{z}_i = \frac{z}{\sqrt{\tilde{n}_i}} = \tilde{s}_i z \quad (i = 1, 2), \tag{11}$$

and $\tilde{n}_i$ $(i = 1, 2)$ are obtained from the following equation,

$$\tilde{c}_{11}\tilde{c}_{44}\tilde{n}_i^2 + \left[\tilde{c}_{13}(\tilde{c}_{13} + 2\tilde{c}_{44}) - \tilde{c}_{11}\tilde{c}_{33}\right]\tilde{n}_i + \tilde{c}_{33}\tilde{c}_{44} = 0, \tag{12}$$

$\tilde{k}_i$ $(i = 1, 2)$ are determined from the following equations:

$$\tilde{n}_i = \frac{\tilde{c}_{44} + (\tilde{c}_{13} + \tilde{c}_{44})\tilde{k}_i}{\tilde{c}_{11}} = \frac{\tilde{c}_{33}\tilde{k}_i}{\tilde{c}_{44}\tilde{k}_i + \tilde{c}_{13} + \tilde{c}_{44}}, \tag{13}$$

where $\tilde{c}_{11}$, $\tilde{c}_{12}$, $\tilde{c}_{13}$, $\tilde{c}_{33}$, $\tilde{c}_{44}$ are the elastic moduli in the elastic medium.

We set up the following boundary conditions including the electric continuous boundary conditions:

$$\sigma_z^{(\mathrm{p})}(r, 0) = 0 \quad (0 \leqslant r < a), \qquad u_z^{(\mathrm{p})}(r, 0) = 0 \quad (a < r < b), \tag{14}$$

$$\begin{aligned} &D_z^{(\mathrm{p})}(r, 0^+) = D_z^{(\mathrm{p})}(r, 0^-) \quad (0 \leqslant r < a), \\ &E_r^{(\mathrm{p})}(r, 0^+) = E_r^{(\mathrm{p})}(r, 0^-) \quad (0 \leqslant r < a), \\ &\phi(r, 0) = 0 \quad (a < r < b), \end{aligned} \tag{15}$$

$$\sigma_{rz}^{(\mathrm{p})}(r, 0) = 0 \quad (0 \leqslant r < b), \tag{16}$$

$$u_r^{(\mathrm{p})}(b, z) = u_r^{(\mathrm{e})}(b, z) \quad (0 \leqslant z < \infty), \tag{17}$$

$$u_z^{(\mathrm{p})}(b, z) = u_z^{(\mathrm{e})}(b, z) \quad (0 \leqslant z < \infty), \tag{18}$$

$$\sigma_r^{(\mathrm{p})}(b, z) = \sigma_r^{(\mathrm{e})}(b, z) \quad (0 \leqslant z < \infty), \tag{19}$$

$$\sigma_{rz}^{(\mathrm{p})}(b, z) = \sigma_{rz}^{(\mathrm{e})}(b, z) \quad (0 \leqslant z < \infty), \tag{20}$$

$$D_r(b, z) = 0 \quad (0 \leqslant z < \infty). \tag{21}$$

There may be the following four possible cases of combined mechanical and electrical loads at infinity,

$$\text{(Case 1)} \quad \sigma_z(r, \infty) = \bar{\sigma}(r), \qquad D_z(r, \infty) = \overline{D}(r), \tag{22}$$

$$\text{(Case 2)} \quad \varepsilon_z(r, \infty) = \bar{\varepsilon}(r), \qquad E_z(r, \infty) = \overline{E}(r), \tag{23}$$

$$\text{(Case 3)} \quad \sigma_z(r, \infty) = \bar{\sigma}(r), \qquad E_z(r, \infty) = \overline{E}(r), \tag{24}$$

$$\text{(Case 4)} \quad \varepsilon_z(r, \infty) = \bar{\varepsilon}(r), \qquad D_z(r, \infty) = \overline{D}(r), \tag{25}$$

where $\bar{\sigma}(r)$, $\bar{\varepsilon}(r)$, $\overline{D}(r)$ and $\overline{E}(r)$ are the magnitudes of applied stress, strain, electric displacement and electric field, respectively.

3. Solution procedure

Applying Hankel transform of order 0 to Eq. (4), we can get the potential functions in the piezoelectric medium in the form,

$$\Phi_i(r, z) = \int_0^\infty \frac{1}{\xi}\left[A_i(\xi) I_0\left(\frac{\xi r}{s_i}\right)\cos(\xi z) + B_i(\xi)\exp(-\xi s_i z) J_0(\xi r)\right] \mathrm{d}\xi, \tag{26}$$

where $A_i(\xi)$ and $B_i(\xi)$ $(i = 1, 2, 3)$ are the unknown functions to be determined by boundary conditions, $J_n(\ )$ is the Bessel function of the first kind of order n and $I_n(\ )$ i s the modified Bessel function of the first kind of order n.

The field equations are obtained in the forms,

$$
\begin{aligned}
u_z^{(\mathrm{p})} &= -\sum_{i=1}^{3} k_{1i} \int_0^\infty A_i(\xi) I_0\left(\frac{\xi r}{s_i}\right) \sin(\xi z)\,\mathrm{d}\xi - \sum_{i=1}^{3} k_{1i} s_i \int_0^\infty B_i(\xi) J_0(\xi r) \exp(-\xi s_i z)\,\mathrm{d}\xi + \bar{a}(r) z, \\
\phi &= \sum_{i=1}^{3} k_{2i} \int_0^\infty A_i(\xi) I_0\left(\frac{\xi r}{s_i}\right) \sin(\xi z)\,\mathrm{d}\xi + \sum_{i=1}^{3} k_{2i} s_i \int_0^\infty B_i(\xi) J_0(\xi r) \exp(-\xi s_i z)\,\mathrm{d}\xi - \bar{b}(r) z, \\
\sigma_z^{(\mathrm{p})} &= -\sum_{i=1}^{3} \frac{F_{1i}}{s_i^2} \int_0^\infty \xi A_i(\xi) I_0\left(\frac{\xi r}{s_i}\right) \cos(\xi z)\,\mathrm{d}\xi + \sum_{i=1}^{3} F_{1i} \int_0^\infty \xi B_i(\xi) J_0(\xi r) \exp(-\xi s_i z)\,\mathrm{d}\xi + \bar{c}(r), \\
\sigma_{rz}^{(\mathrm{p})} &= -\sum_{i=1}^{3} \frac{F_{3i}}{s_i^2} \int_0^\infty \xi A_i(\xi) I_1\left(\frac{\xi r}{s_i}\right) \sin(\xi z)\,\mathrm{d}\xi + \sum_{i=1}^{3} F_{3i} \int_0^\infty \xi B_i(\xi) J_1(\xi r) \exp(-\xi s_i z)\,\mathrm{d}\xi, \\
D_z &= -\sum_{i=1}^{3} \frac{F_{2i}}{s_i^2} \int_0^\infty \xi A_i(\xi) I_0\left(\frac{\xi r}{s_i}\right) \cos(\xi z)\,\mathrm{d}\xi + \sum_{i=1}^{3} F_{2i} \int_0^\infty \xi B_i(\xi) J_0(\xi r) \exp(-\xi s_i z)\,\mathrm{d}\xi + \bar{d}(r),
\end{aligned}
\tag{27}
$$

where

$$
\begin{aligned}
&F_{1i} = (c_{33} k_{1i} - e_{33} k_{2i}) s_i^2 - c_{13}, \quad F_{2i} = (e_{33} k_{1i} + d_{33} k_{2i}) s_i^2 - e_{31}, \\
&F_{3i} = [c_{44}(1 + k_{1i}) - e_{15} k_{2i}] s_i, \qquad (i = 1, 2, 3),
\end{aligned}
\tag{28}
$$

and $\bar{a}(r)$, $\bar{b}(r)$, $\bar{c}(r) = c_{33}\bar{a}(r) - e_{33}\bar{b}(r)$ and $\bar{d}(r) = e_{33}\bar{a}(r) + d_{33}\bar{b}(r)$ are the unknown functions to be determined from the applied loading conditions.

Similarly, we can get the potential functions in the elastic medium in the form,

$$
\widetilde{\Phi}_i(r, z) = \int_0^\infty \frac{1}{\xi} C_i(\xi) K_0\left(\frac{\xi r}{\tilde{s}_i}\right) \cos(\xi z)\,\mathrm{d}\xi,
\tag{29}
$$

where $C_i(\xi)$ $(i = 1, 2)$ are the unknown functions to be determined by boundary conditions, and $K_n(\ )$ is the modified Bessel function of the second kind of order n.

The field equations are in the elastic medium obtained in the forms,

$$
\begin{aligned}
u_z^{(\mathrm{e})} &= -\sum_{i=1}^{2} \tilde{k}_i \int_0^\infty C_i(\xi) K_0\left(\frac{\xi r}{\tilde{s}_i}\right) \sin(\xi z)\,\mathrm{d}\xi, \\
u_r^{(\mathrm{e})} &= -\sum_{i=1}^{2} \frac{1}{\tilde{s}_i} \int_0^\infty C_i(\xi) K_1\left(\frac{\xi r}{\tilde{s}_i}\right) \cos(\xi z)\,\mathrm{d}\xi, \\
\sigma_r^{(\mathrm{e})} &= \frac{\tilde{c}_{11}}{2} \sum_{i=1}^{2} \frac{1}{\tilde{s}_i^2} \int_0^\infty \xi C_i(\xi) \left[K_0\left(\frac{\xi r}{\tilde{s}_i}\right) + K_2\left(\frac{\xi r}{\tilde{s}_i}\right)\right] \cos(\xi z)\,\mathrm{d}\xi \\
&\quad - \tilde{c}_{13} \sum_{i=1}^{2} \tilde{k}_i \int_0^\infty \xi C_i(\xi) K_0\left(\frac{\xi r}{\tilde{s}_i}\right) \cos(\xi z)\,\mathrm{d}\xi, \\
\sigma_{rz}^{(\mathrm{e})} &= \sum_{i=1}^{2} \frac{\widetilde{F}_{2i}}{\tilde{s}_i^2} \int_0^\infty \xi C_i(\xi) K_1\left(\frac{\xi r}{\tilde{s}_i}\right) \sin(\xi z)\,\mathrm{d}\xi,
\end{aligned}
\tag{30}
$$

where

$$
\widetilde{F}_{1i} = \tilde{c}_{33} \tilde{k}_i \tilde{s}_i^2 - \tilde{c}_{13}, \quad \widetilde{F}_{2i} = \tilde{c}_{44}(1 + \tilde{k}_i) \tilde{s}_i \qquad (i = 1, 2).
\tag{31}
$$

Eqs. (22)–(25), the following coefficients are obtained:

$$\text{(Case 1)}\quad \bar{a}(r)=\frac{d_{33}\bar{\sigma}(r)+e_{33}\overline{D}(r)}{c_{33}d_{33}+e_{33}^2},\qquad \bar{b}(r)=\frac{c_{33}\overline{D}(r)-e_{33}\bar{\sigma}(r)}{c_{33}d_{33}+e_{33}^2},\qquad \bar{c}(r)=\bar{\sigma}(r),\qquad \bar{d}(r)=\overline{D}(r), \tag{32}$$

$$\text{(Case 2)}\quad \bar{a}(r)=\bar{\varepsilon}(r),\qquad \bar{b}(r)=\overline{E}(r),\qquad \bar{c}(r)=c_{33}\bar{\varepsilon}(r)-e_{33}\overline{E}(r),\qquad \bar{d}(r)=e_{33}\bar{\varepsilon}(r)+d_{33}\overline{E}(r), \tag{33}$$

$$\text{(Case 3)}\quad \bar{a}(r)=\frac{\bar{\sigma}(r)+e_{33}\overline{E}(r)}{c_{33}},\qquad \bar{b}(r)=\overline{E}(r),\qquad \bar{c}(r)=\bar{\sigma}(r),\qquad \bar{d}(r)=\frac{e_{33}\bar{\sigma}(r)+(c_{33}d_{33}+e_{33}^2)\overline{E}(r)}{c_{33}}, \tag{34}$$

$$\text{(Case 4)}\quad \bar{a}(r)=\bar{\varepsilon}(r),\qquad \bar{b}(r)=\frac{\overline{D}(r)-e_{33}\bar{\varepsilon}(r)}{d_{33}},\qquad \bar{c}(r)=\frac{(c_{33}d_{33}+e_{33}^2)\bar{\varepsilon}(r)-e_{33}\overline{D}(r)}{d_{33}},\qquad \bar{d}(r)=\overline{D}(r). \tag{35}$$

From Eqs. (15)–(21), (27) and (30), the following relations between the coefficients are obtained,

$$B_2(\xi)=M_2B_1(\xi),\qquad B_3(\xi)=M_3B_1(\xi),$$

$$\begin{aligned}A_1(\xi)=\frac{1}{\Delta(\xi)}\sum_{i=1}^{3}\Big\{&M_i(F_{4i}[h_{22}(\xi)h_{33}(\xi)-h_{23}(\xi)h_{32}(\xi)]+h_{4i}(\xi)[h_{13}(\xi)h_{32}(\xi)-h_{12}(\xi)h_{33}(\xi)]\\&+h_{5i}(\xi)[h_{12}(\xi)h_{23}(\xi)-h_{13}(\xi)h_{22}(\xi)])f_{1i}(\xi)+M_i\xi h_{6i}[h_{13}(\xi)h_{32}(\xi)-h_{12}(\xi)h_{33}(\xi)]f_{2i}(\xi)\\&+\frac{M_i}{\xi}h_{7i}[h_{12}(\xi)h_{23}(\xi)-h_{13}(\xi)h_{22}(\xi)]f_{3i}(\xi)+\frac{M_i}{\xi}h_{8i}[h_{12}(\xi)h_{23}(\xi)-h_{13}(\xi)h_{22}(\xi)]f_{4i}(\xi)\Big\},\end{aligned}$$

$$\begin{aligned}A_2(\xi)=\frac{1}{\Delta(\xi)}\sum_{i=1}^{3}\Big\{&M_i(F_{4i}[h_{23}(\xi)h_{31}(\xi)-h_{21}(\xi)h_{33}(\xi)]+h_{4i}(\xi)[h_{11}(\xi)h_{33}(\xi)-h_{13}(\xi)h_{31}(\xi)]\\&+h_{5i}(\xi)[h_{13}(\xi)h_{21}(\xi)-h_{11}(\xi)h_{23}(\xi)])f_{1i}(\xi)+M_i\xi h_{6i}[h_{11}(\xi)h_{33}(\xi)-h_{13}(\xi)h_{31}(\xi)]f_{2i}(\xi)\\&+\frac{M_i}{\xi}h_{7i}[h_{13}(\xi)h_{21}(\xi)-h_{11}(\xi)h_{23}(\xi)]f_{3i}(\xi)+\frac{M_i}{\xi}h_{8i}[h_{13}(\xi)h_{21}(\xi)-h_{11}(\xi)h_{23}(\xi)]f_{4i}(\xi)\Big\},\end{aligned}$$

$$\begin{aligned}A_3(\xi)=\frac{1}{\Delta(\xi)}\sum_{i=1}^{3}\Big\{&M_i(F_{4i}[h_{21}(\xi)h_{32}(\xi)-h_{22}(\xi)h_{31}(\xi)]+h_{4i}(\xi)[h_{12}(\xi)h_{31}(\xi)-h_{11}(\xi)h_{32}(\xi)]\\&+h_{5i}(\xi)[h_{11}(\xi)h_{22}(\xi)-h_{12}(\xi)h_{21}(\xi)])f_{1i}(\xi)+M_i\xi h_{6i}[h_{12}(\xi)h_{31}(\xi)-h_{11}(\xi)h_{32}(\xi)]f_{2i}(\xi)\\&+\frac{M_i}{\xi}h_{7i}[h_{11}(\xi)h_{22}(\xi)-h_{12}(\xi)h_{21}(\xi)]f_{3i}(\xi)+\frac{M_i}{\xi}h_{8i}[h_{11}(\xi)h_{22}(\xi)-h_{12}(\xi)h_{21}(\xi)]f_{4i}(\xi)\Big\},\end{aligned}$$

$$C_1(\xi)=\frac{1}{K_1(\xi b/\tilde{s}_1)}\sum_{i=1}^{3}\left\{g_{1i}I_1\left(\frac{\xi b}{s_i}\right)A_i(\xi)+M_ig_{2i}f_{1i}(\xi)\right\},$$

$$C_2(\xi)=\frac{1}{K_1(\xi b/\tilde{s}_2)}\sum_{i=1}^{3}\left\{g_{3i}I_1\left(\frac{\xi b}{s_i}\right)A_i(\xi)+M_ig_{4i}f_{1i}(\xi)\right\}, \tag{36}$$

where

$$M_1 = 1, \qquad M_2 = \frac{F_{31}k_{23}s_3 - F_{33}k_{21}s_1}{F_{33}k_{22}s_2 - F_{32}k_{23}s_3}, \qquad M_3 = \frac{F_{32}k_{21}s_1 - F_{31}k_{22}s_2}{F_{33}k_{22}s_2 - F_{32}k_{23}s_3},$$

$$\begin{aligned}\Delta(\xi) &= h_{11}(\xi)[h_{22}(\xi)h_{33}(\xi) - h_{23}(\xi)h_{32}(\xi)] + h_{12}(\xi)[h_{23}(\xi)h_{31}(\xi) - h_{21}(\xi)h_{33}(\xi)] \\ &\quad + h_{13}(\xi)[h_{21}(\xi)h_{32}(\xi) - h_{22}(\xi)h_{31}(\xi)],\end{aligned}$$

$$f_{1i}(\xi) = \frac{2}{\pi}\int_0^\infty \frac{\eta B_1(\eta)J_1(\eta b)}{\eta^2 s_i^2 + \xi^2}\,\mathrm{d}\eta, \qquad f_{2i}(\xi) = \frac{2}{\pi}\int_0^\infty \frac{B_1(\eta)J_0(\eta b)}{\eta^2 s_i^2 + \xi^2}\,\mathrm{d}\eta, \tag{37}$$

$$f_{3i}(\xi) = \frac{2}{\pi}\int_0^\infty \frac{\eta^2 B_1(\eta)J_0(\eta b)}{\eta^2 s_i^2 + \xi^2}\,\mathrm{d}\eta, \qquad f_{4i}(\xi) = \frac{2}{\pi}\int_0^\infty \frac{\eta^2 B_1(\eta)J_2(\eta b)}{\eta^2 s_i^2 + \xi^2}\,\mathrm{d}\eta,$$

$$F_{4i} = [e_{15}(1 + k_{1i}) + d_{11}k_{2i}]s_i,$$

and the quantities $h_{ji}(\xi)$ ($j = 1$–5, $i = 1$–3), h_{ji} ($j = 6$–8, $i = 1$–3) and g_{ji} ($j = 1$–4, $i = 1$–3) are given by Eq. (A.1) in Appendix A.

From Eq. (14), a system of dual integral equation is obtained,

$$\begin{aligned}&-\int_0^\infty \xi\left[\frac{F_{11}}{s_1^2}I_0\left(\frac{\xi r}{s_1}\right)A_1(\xi) + \frac{F_{12}}{s_2^2}I_0\left(\frac{\xi r}{s_2}\right)A_2(\xi) + \frac{F_{13}}{s_3^2}I_0\left(\frac{\xi r}{s_3}\right)A_3(\xi)\right]\mathrm{d}\xi \\ &\quad + \int_0^\infty \xi[M_1F_{11} + M_2F_{12} + M_3F_{13}]B_1(\xi)J_0(\xi r)\,\mathrm{d}\xi = -\bar{c}(r) \quad (0 \leqslant r < a), \\ &\int_0^\infty [M_1k_{11}s_1 + M_2k_{12}s_2 + M_3k_{13}s_3]B_1(\xi)J_0(\xi r)\,\mathrm{d}\xi = 0 \quad (a < r < b).\end{aligned} \tag{38}$$

Eq. (38) may be solved by using the function $\psi(\alpha)$ defined by

$$B_1(\xi) = \int_0^a \psi(\alpha)\sin(\xi\alpha)\,\mathrm{d}\alpha, \tag{39}$$

where $\psi(0) = 0$.

Inserting Eqs. (36), (37) and (39) into Eq. (38), we obtain a Fredholm integral equation of the second kind in the form,

$$\psi(\alpha) + \int_0^a \psi(\beta)L(\alpha,\beta)\,\mathrm{d}\beta = \frac{2}{\pi m_0}\int_0^\alpha \frac{r\bar{c}(r)}{\sqrt{\alpha^2 - r^2}}\,\mathrm{d}r, \tag{40}$$

where

$$m_0 = -(M_1F_{11} + M_2F_{12} + M_3F_{13}), \tag{41}$$

and $L(\alpha,\beta)$ is given by Eq. (B.1) in Appendix B.

Each kind of the field intensity factors is obtained in the form,

$$K^\sigma = K_I = \lim_{r\to a^+}\sqrt{2\pi(r-a)}\sigma_z(r,0) = \sqrt{\frac{\pi}{a}}m_0\psi(a), \tag{42}$$

$$K^D = \lim_{r\to a^+}\sqrt{2\pi(r-a)}D_z(r,0) = \sqrt{\frac{\pi}{a}}m_1\psi(a), \tag{43}$$

$$K^\varepsilon = \lim_{r\to a^+}\sqrt{2\pi(r-a)}\varepsilon_z(r,0) = \sqrt{\frac{\pi}{a}}m_2\psi(a), \tag{44}$$

$$K^E = \lim_{r\to a^+} \sqrt{2\pi(r-a)}E_z(r,0) = \sqrt{\frac{\pi}{a}}m_3\psi(a), \tag{45}$$

where

$$\begin{aligned} m_1 &= -[F_{21}M_1 + F_{22}M_2 + F_{23}M_3], \\ m_2 &= -[k_{11}s_1^2M_1 + k_{12}s_2^2M_2 + k_{13}s_3^2M_3], \\ m_3 &= -[k_{21}s_1^2M_1 + k_{22}s_2^2M_2 + k_{23}s_3^2M_3], \end{aligned} \tag{46}$$

and K^σ, K^D, K^ε and K^E are the stress intensity factor, electric displacement intensity factor, strain intensity factor and electric field intensity factor, respectively.

4. Numerical results and discussion

Material properties of PZT-6B ceramic are as follows (Wang and Huang, 1995; Wang and Zheng, 1995),

elastic constants (10^{10} N/m^2): $c_{11} = 16.8$, $c_{12} = 6.0$, $c_{13} = 6.0$, $c_{33} = 16.3$, $c_{44} = 2.71$;
piezoelectric constants (C/m^2): $e_{15} = 4.6$, $e_{31} = -0.9$, $e_{33} = 7.1$;
dielectric permittivities (10^{-10} F/m): $d_{11} = 36$, $d_{33} = 34$;

and the material properties of several elastic media are shown in Table 1.

4.1. Example 1. Uniform loads

Let the following loads be applied:

$$\begin{aligned} &\sigma_z(r,\infty) = \sigma_0 \quad \text{(for Cases 1 and 3)}, \\ &\varepsilon_z(r,\infty) = \varepsilon_0 \quad \text{(for Cases 2 and 4)}, \\ &D_z(r,\infty) = -D_0, \quad \text{(for Cases 1 and 4)}, \\ &E_z(r,\infty) = -E_0, \quad \text{(for Cases 2 and 3)}, \end{aligned} \tag{47}$$

where σ_0, ε_0, D_0 and E_0 are the magnitudes of applied constant stress, strain, electric displacement and electric field, respectively. "−" in Eq. (47) means that the electric loading directions are the same as the poling direction as shown in Fig. 1. In this case, a Fredholm integral equation of the second kind is obtained from Eq. (40) in the form,

$$\Psi(\Xi) + \int_0^1 \Psi(H)K(\Xi,H)\,\mathrm{d}H = \Xi, \tag{48}$$

Table 1
The material properties of elastic medium (10^{10} N/m^2)

Material	Elastic constants				
	c_{11}	c_{12}	c_{13}	c_{33}	c_{44}
Boron-epoxy	2.94	1.37	2.46	20.89	0.81
Graphite epoxy	0.83	0.28	0.03	8.68	0.42
E-glass epoxy	1.49	0.66	0.52	4.73	0.48

where

$$K(\Xi,H)=aL(a\Xi,aH),\qquad \Xi=\frac{\alpha}{a},\quad H=\frac{\beta}{a},\quad \Psi(x)=\frac{\pi}{2}\frac{m_0}{c_0 a}\psi(ax), \tag{49}$$

$$\begin{aligned} c_0 &= \sigma_0 \quad \text{(Cases 1 and 3)}\\ &= c_{33}\varepsilon_0+e_{33}E_0 \quad \text{(Case 2)}\\ &= \frac{(c_{33}d_{33}+e_{33}^2)\varepsilon_0+e_{33}D_0}{d_{33}} \quad \text{(Case 4)}. \end{aligned} \tag{50}$$

The field intensity factors become as follows:

$$K^{\sigma}=\frac{2}{\pi}\sqrt{\pi a}c_0\Psi(1), \tag{51}$$

$$K^{D}=\frac{2}{\pi}\sqrt{\pi a}\frac{m_1}{m_0}c_0\Psi(1), \tag{52}$$

$$K^{\varepsilon}=\frac{2}{\pi}\sqrt{\pi a}\frac{m_2}{m_0}c_0\Psi(1), \tag{53}$$

$$K^{E}=\frac{2}{\pi}\sqrt{\pi a}\frac{m_3}{m_0}c_0\Psi(1). \tag{54}$$

Eq. (48) is solved numerically using Gaussian quadrature formula. From the above equations we can conclude that in Case 1 the stress intensity factor is dependent on the mechanical load, and the electric displacement intensity factor depends on the material properties and the mechanical load, but not on the electrical load. These tendencies are consistent with those of Gao and Fan (1999a) in two-dimensional mixed mode problem and those of Yang and Lee (2001) in three-dimensional opening mode problem. Also the field intensity factors are independent upon the electrical loads under constant stress loads (Cases 1 and 3), but dependent upon them under constant strain loads (Cases 2 and 4). These results agree with those of Shindo et al. (1997) and Zhang and Hack (1992) in two-dimensional mode III problem.

The change of the normalized stress intensity factor for Case 1 according to the ratio of crack radius to PZT-6B piezoelectric cylinder radius and various elastic media under uniform loads are shown in Fig. 2. The normalized stress intensity factor increases with increase of the ratio a/b for graphite epoxy and E-glass epoxy, but it decreases for boron-epoxy.

According to Satapathy and Parhi (1979), the similar behavior of stress intensity factor is obtained in the crack problem for an elastic cylinder surrounded by an another elastic infinite medium. They showed that the stress intensity factor may increase or decrease according to the ratio of crack radius to cylinder radius with the combination of inside and outside materials. From the observation for the effect of various material properties in our piezoelectric problem, we find out that c_{33} only affects the increase or decrease of the stress intensity factor with the variation of the ratio of the crack radius to the cylinder radius. Fig 3 shows that the stress intensity factor increases with increase of the ratio a/b when c_{33} of the inside piezoelectric medium is larger than $\tilde{c}_{33}$ of the outside elastic medium. Even though c_{44} affects the increase or decrease of the stress intensity factor in mode III problem (Sih and Chen, 1981), in model I problem c_{33} does.

The variations of the normalized field intensity factors for Case 1 according to the ratio of crack radius to PZT-6B piezoelectric cylinder radius in the case surrounded by graphite epoxy under uniform loads are shown in Fig. 4. It is shown that the normalized field intensity factors increase with increase of the ratio

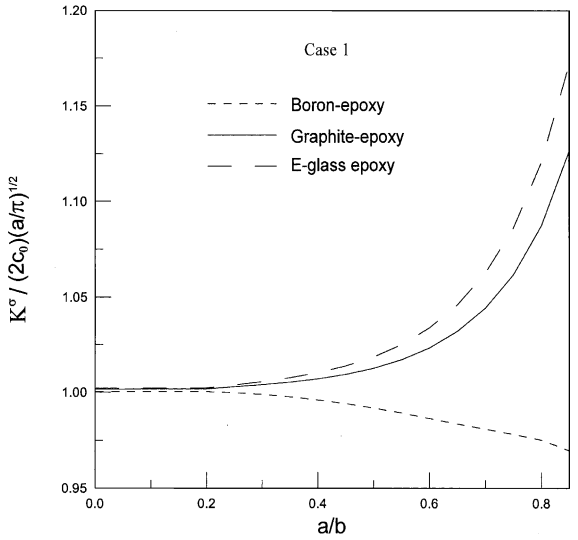

Fig. 2. Change of the normalized stress intensity factor with the ratio of crack radius to PZT-6B cylinder radius and several elastic media under uniform loads in Case 1.

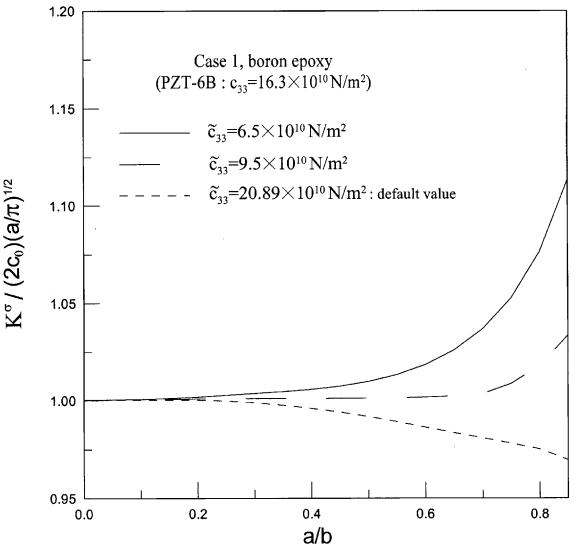

Fig. 3. Change of the normalized stress intensity factor with the ratio of crack radius to PZT-6B cylinder radius and $\tilde{c}_{33}$ of the boron epoxy under uniform loads in Case 1.

a/b, and it is noted that the stress intensity factor and the electric field intensity factor are much larger than the strain intensity factor and the electric displacement intensity factor.

Fig. 5 shows the change of $K^\sigma/2(a/\pi)^{1/2}$ with the applied electric field E_0 and the ratio a/b in the case surrounded by graphite epoxy under uniform loads. It is noted that the crack size affects a little to the stress intensity factor in case of electric loading alone. And it is concluded from Fig. 5 that cracks may or not propagate according to the direction and value of the applied electric field. This tendency is different from

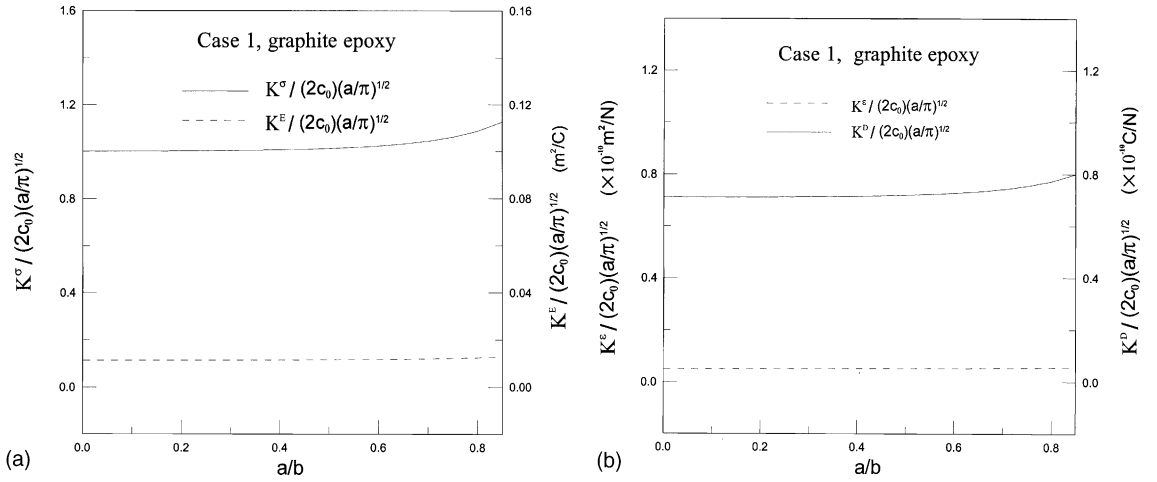

Fig. 4. Change of the normalized field intensity factors with the ratio of crack radius to PZT-6B cylinder radius in the case surrounded by graphite epoxy under uniform loads in Case 1.

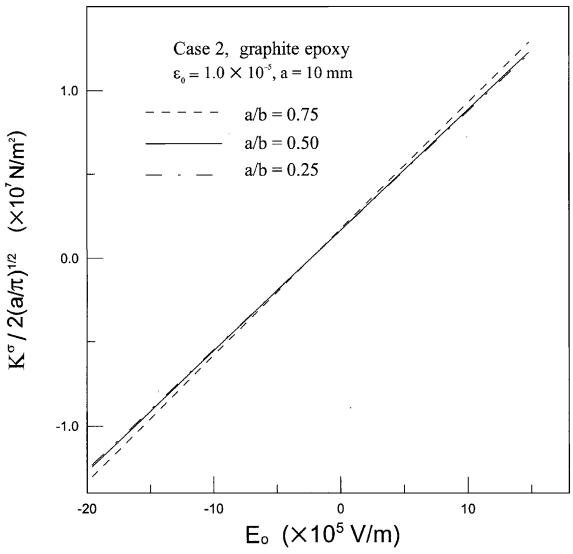

Fig. 5. Change of normalized stress intensity factor $K^{\sigma}/2(a/\pi)^{1/2}$ with the applied electrical field E_0 in case of PZT-6B ceramic and graphite epoxy under uniform loads in Case 2.

the results of the electric impermeable condition on the crack surface (Pak, 1990), and agrees with the experimental observations presented by Park and Sun (1995b).

Park and Sun (1995b) got the stress intensity factor, the total energy release rate and the mechanical strain energy release rate for a crack with the electric impermeable condition in an infinite piezoelectric medium for the three fracture mode theoretically and the experimentally. Their analytic results showed that the electric loading alone cannot affect the stress intensity factor and the total energy release rate becomes

negative, and they insisted that the stress intensity factor and the total energy release rate are not suitable for describing the fracture behavior of piezoelectric ceramics. But it is important to remember that those results were caused by the electrical impermeable condition on the crack surfaces.

The tendency of the variation of the stress intensity factor with the applied electric displacement D_0 in Case 4 were observed to the similar with that with the electric field in Case 2.

4.2. Example 2. Ring-shaped load

Let normal loading per a unit area, p apply on the region of $r_1 \leqslant r \leqslant r_2$, $0^\circ \leqslant \theta \leqslant 360^\circ$ and the electrical loads be arbitrary as shown in Fig. 6. Then, the applied loads can be expressed as follows:

$$\begin{aligned} &\sigma_z(r,\infty) = \begin{cases} p, & \text{for } r_1 \leqslant r \leqslant r_2, \\ 0, & \text{elsewhere,} \end{cases} \quad \text{(for Cases 1 and 3)}, \\ &D_z(r,\infty) = \overline{D}(r), \quad \text{(for Case 1)}, \\ &E_z(r,\infty) = \overline{E}(r), \quad \text{(for Case 3)}. \end{aligned} \tag{55}$$

Using Eqs. (32), (34) and (55), a Fredholm integral equation of the second kind is obtained from Eq. (40) in the form,

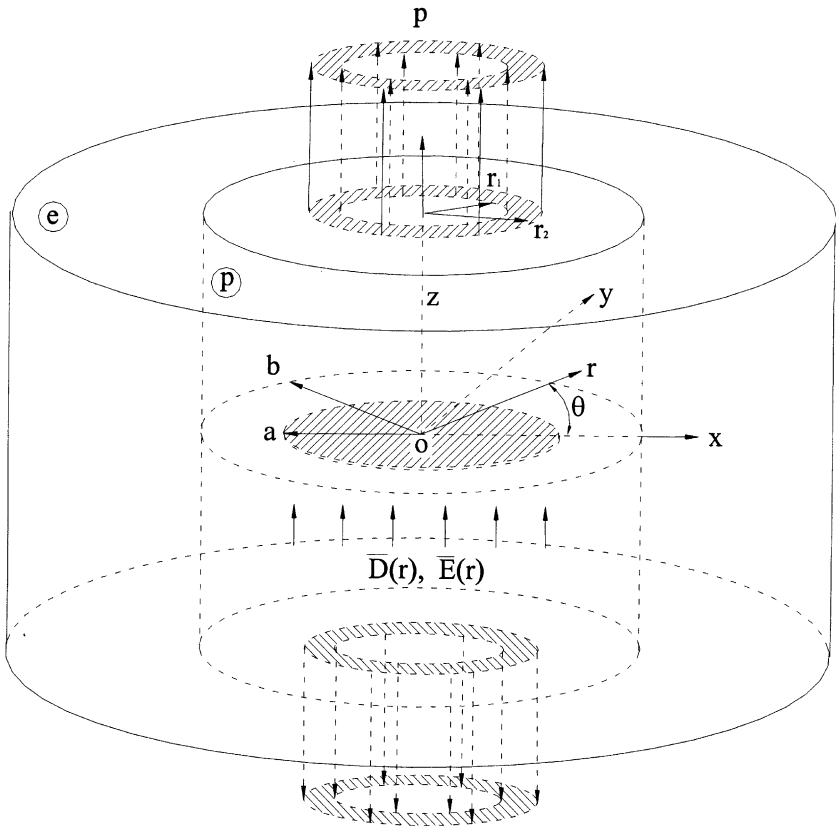

Fig. 6. Piezoelectric cylinder with a penny shaped crack surrounded by an infinite elastic medium under a ring-shaped normal mechanical load and general electrical load.

$$\Psi(\Xi) + \int_0^1 \Psi(H)K(\Xi, H)\,\mathrm{d}H = \Xi, \tag{56}$$

where

$$\Xi = \frac{\alpha}{a}, \qquad H = \frac{\beta}{a}, \qquad \Psi(x) = \frac{\pi}{2}\frac{m_0}{pa}\frac{1}{\sqrt{1-(r_1/\alpha)^2} - \sqrt{1-(r_2/\alpha)^2}}\psi(ax), \tag{57}$$

and the kernel $K(\Xi, H)$ is the same as Example 1.

The field intensity factors become as follows:

$$K^{\sigma} = \frac{2}{\pi}\sqrt{\pi a}p\left(\sqrt{1-a_1^2} - \sqrt{1-a_2^2}\right)\Psi(1), \tag{58}$$

$$K^{D} = \frac{2}{\pi}\sqrt{\pi a}\frac{m_1}{m_0}p\left(\sqrt{1-a_1^2} - \sqrt{1-a_2^2}\right)\Psi(1), \tag{59}$$

$$K^{\varepsilon} = \frac{2}{\pi}\sqrt{\pi a}\frac{m_2}{m_0}p\left(\sqrt{1-a_1^2} - \sqrt{1-a_2^2}\right)\Psi(1), \tag{60}$$

$$K^{E} = \frac{2}{\pi}\sqrt{\pi a}\frac{m_3}{m_0}p\left(\sqrt{1-a_1^2} - \sqrt{1-a_2^2}\right)\Psi(1), \tag{61}$$

where $a_1 = r_1/a$ and $a_2 = r_2/a$.

The Fredholm integral equation is solved numerically by the same method as Example 1. Various field intensity factors are obtained from Eqs. (58)–(61). In this example, only Cases 1 and 3 are considered and the results that the field intensity factors are not affected from the applied electrical loads are obtained.

Fig. 7 shows the variation of the normalized stress intensity factor with the ratio of crack radius to cylinder radius a/b under a ring-shaped mechanical load ($a_2 - a_1 = 0.1$) and an arbitrary electrical load in

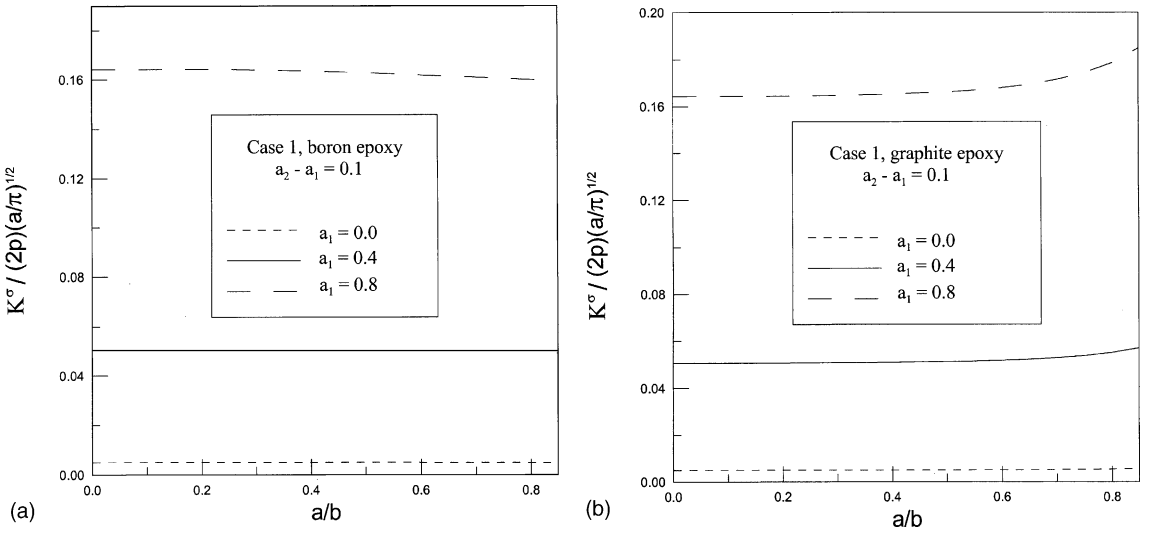

Fig. 7. Change of the normalized stress intensity factor with the ratio of crack radius to PZT-6B cylinder radius under a ring-shaped mechanical load ($a_2 - a_1 = 0.1$) and an arbitrary electrical load in Case 1.

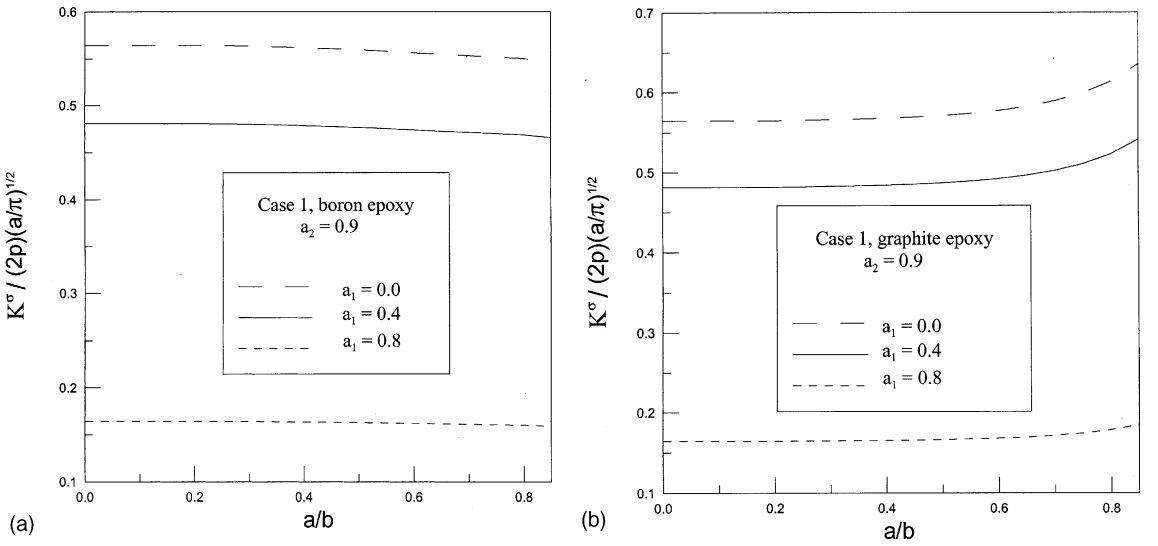

Fig. 8. Change of the normalized stress intensity factor with the ratio of crack radius to PZT-6B cylinder radius under a ring-shaped mechanical load ($a_2 = 0.9$, $a_1 = 0.0, 0.4, 0.8$) and an arbitrary electrical load in Case 1.

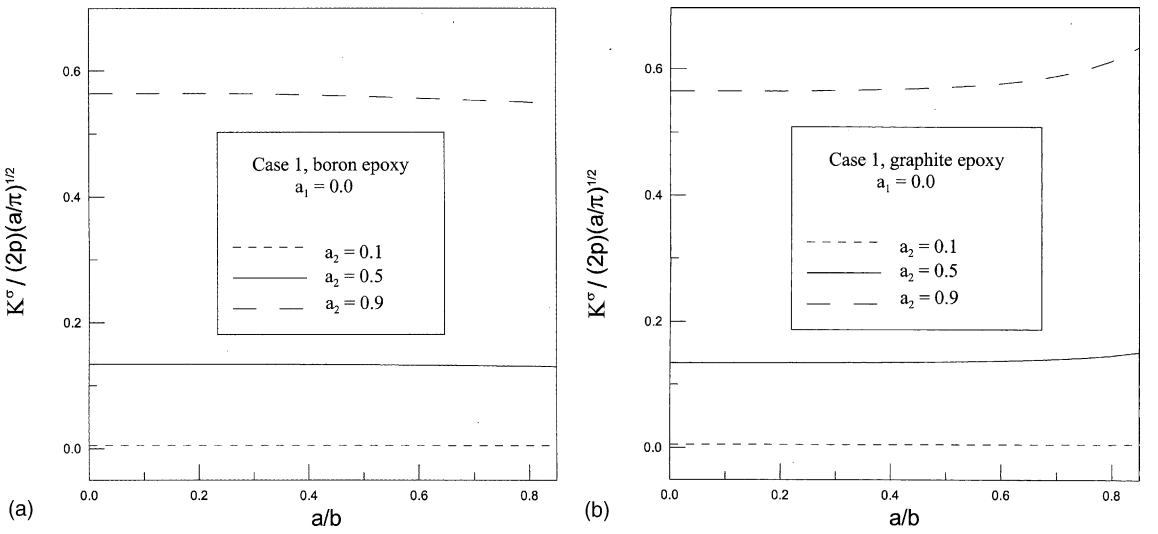

Fig. 9. Change of the normalized stress intensity factor with the ratio of crack radius to PZT-6B cylinder radius under a circular mechanical load and an arbitrary electrical load in Case 1.

Case 1. The normalized stress intensity factor decreases with increase of the ratio a/b in case of boron epoxy and increases with increase of a/b in case of graphite epoxy, and the value increases as the position of the applied load approaches near the crack border.

The changes of the normalized stress intensity factor with the ratio of crack radius to cylinder radius a/b under a ring-shaped mechanical load ($a_2 = 0.9$, $a_1 = 0.0, 0.4, 0.8$) and an arbitrary electrical load in Case 1 are shown in Fig. 8. As the value of a_1 decreases, the normalized stress intensity factor increases. When the

value of a_1 becomes from 0.8 to 0.4, the normalized stress intensity factor increases very much, but when that becomes from 0.4 to 0.0, the value increases a little. This implies that the load apart from the crack border affects the normalized stress intensity factor a little.

Fig. 9 shows the variation of the normalized stress intensity factor with the ratio of crack radius to cylinder radius a/b under a circular mechanical load and an arbitrary electrical load in Case 1. It is the limiting case as a_1 becomes 0. Also as the area of the applied load increase, the normalized stress intensity factor increases. And as a_2 becomes near 1.0, the stress intensity factor increases very much.

5. Conclusions

The solutions of the field equations and the field intensity factors for a penny shaped crack in a transversely isotropic piezoelectric ceramic cylinder surrounded by an infinite elastic medium under in-plane mechanical and electrical loads are obtained by the potential theory and the integral transform method. The continuous electric boundary conditions are used on the crack surfaces and the justification of them are discussed. Various field intensity factors are obtained from the solution of a Fredholm integral equation of the second kind, and the field intensity factors under the uniform mechanical and electrical loads as well as a ring-shaped mechanical load with an arbitrary electrical load are shown numerically. The tendency of the field intensity factors with the ratio of crack radius to cylinder radius is different for the various elastic medium. When the boron-epoxy is used, the field intensity factors decrease with increase of the ratio of crack radius to cylinder radius. But, the tendency is opposite for graphite-epoxy and E-glass epoxy. This behavior is due to the ratio of material properties $c_{33}/\tilde{c}_{33}$ (inside medium/outside medium). Therefore, we can reduce the fracture of the electric equipments by selecting the surrounded elastic material properly.

The stress intensity factor may increase or decrease according to the electric loading condition in Cases 2 and 4, and this tendency agnrees with the previous experimental results (Park and Sun, 1995b).

Appendix A

The $h_{ji}(\xi)$ ($j = 1$–5, $i = 1$–3), h_{ji} ($j = 6$–8, $i = 1$–3) and g_{ji} ($j = 1$–4, $i = 1$–3) in Eq. (36) are as follows:

$$h_{1i}(\xi) = \frac{F_{4i}}{s_i^2} I_1\left(\frac{\xi b}{s_i}\right),$$

$$h_{2i}(\xi) = k_{1i} I_0\left(\frac{\xi b}{s_i}\right) - \tilde{k}_1 g_{1i} I_1\left(\frac{\xi b}{s_i}\right) K_0\left(\frac{\xi b}{\tilde{s}_1}\right) \Big/ K_1\left(\frac{\xi b}{\tilde{s}_1}\right) - \tilde{k}_2 g_{3i} I_1\left(\frac{\xi b}{s_i}\right) K_0\left(\frac{\xi b}{\tilde{s}_2}\right) \Big/ K_1\left(\frac{\xi b}{\tilde{s}_2}\right),$$

$$h_{3i}(\xi) = \frac{F_{5i}}{s_i^2} I_0\left(\frac{\xi b}{s_i}\right) - \frac{c_{11}}{2s_i^2} I_2\left(\frac{\xi b}{s_i}\right) - \frac{\widetilde{F}_{31}}{\tilde{s}_1^2} g_{1i} I_1\left(\frac{\xi b}{s_i}\right) K_0\left(\frac{\xi b}{\tilde{s}_1}\right) \Big/ K_1\left(\frac{\xi b}{\tilde{s}_1}\right) + \frac{\tilde{c}_{11}}{2\tilde{s}_1^2} g_{1i} I_1\left(\frac{\xi b}{s_i}\right) K_2\left(\frac{\xi b}{\tilde{s}_1}\right) \Big/ K_1\left(\frac{\xi b}{\tilde{s}_1}\right) - \frac{\widetilde{F}_{32}}{\tilde{s}_2^2} g_{3i} I_1\left(\frac{\xi b}{s_i}\right) K_0\left(\frac{\xi b}{\tilde{s}_2}\right) \Big/ K_1\left(\frac{\xi b}{\tilde{s}_2}\right) + \frac{\tilde{c}_{11}}{2\tilde{s}_2^2} g_{3i} I_1\left(\frac{\xi b}{s_i}\right) K_2\left(\frac{\xi b}{\tilde{s}_2}\right) \Big/ K_1\left(\frac{\xi b}{\tilde{s}_2}\right),$$

$$
\begin{aligned}
h_{4i}(\xi) &= \tilde{k}_1 g_{2i} K_0\left(\frac{\xi b}{\tilde{s}_1}\right)\Big/ K_1\left(\frac{\xi b}{\tilde{s}_1}\right) + \tilde{k}_2 g_{4i} K_0\left(\frac{\xi b}{\tilde{s}_2}\right)\Big/ K_1\left(\frac{\xi b}{\tilde{s}_2}\right),\\
h_{5i}(\xi) &= \frac{\widetilde{F}_{31}}{\tilde{s}_1^2} g_{2i} K_0\left(\frac{\xi b}{\tilde{s}_1}\right)\Big/ K_1\left(\frac{\xi b}{\tilde{s}_1}\right) - \frac{\tilde{c}_{11}}{2\tilde{s}_1^2} g_{2i} K_2\left(\frac{\xi b}{\tilde{s}_1}\right)\Big/ K_1\left(\frac{\xi b}{\tilde{s}_1}\right)\\
&\quad + \frac{\widetilde{F}_{32}}{\tilde{s}_2^2} g_{4i} K_0\left(\frac{\xi b}{\tilde{s}_2}\right)\Big/ K_1\left(\frac{\xi b}{\tilde{s}_2}\right) - \frac{\tilde{c}_{11}}{2\tilde{s}_2^2} g_{4i} K_2\left(\frac{\xi b}{\tilde{s}_2}\right)\Big/ K_1\left(\frac{\xi b}{\tilde{s}_2}\right),\\
h_{6i} &= -k_{1i} s_i, \qquad h_{7i} = F_{5i} s_i, \qquad h_{8i} = -\frac{c_{11}}{2} s_i,\\
g_{1i} &= \frac{1}{\tilde{c}_{44}(\tilde{k}_2 - \tilde{k}_1)} \frac{\tilde{s}_1}{s_i}\left(\frac{F_{3i}}{s_i} - \frac{\widetilde{F}_{22}}{\tilde{s}_2}\right), \qquad g_{2i} = \frac{1}{\tilde{c}_{44}(\tilde{k}_2 - \tilde{k}_1)} \frac{\tilde{s}_1}{\tilde{s}_2}(s_i \widetilde{F}_{22} - \tilde{s}_2 F_{3i}),\\
g_{3i} &= \frac{1}{\tilde{c}_{44}(\tilde{k}_2 - \tilde{k}_1)} \frac{\tilde{s}_2}{s_i}\left(\frac{\widetilde{F}_{21}}{\tilde{s}_1} - \frac{F_{3i}}{s_i}\right), \qquad g_{4i} = \frac{1}{\tilde{c}_{44}(\tilde{k}_2 - \tilde{k}_1)} \frac{\tilde{s}_2}{\tilde{s}_1}(\tilde{s}_1 F_{3i} - s_i \widetilde{F}_{21}),
\end{aligned}
\tag{A.1}
$$

where

$$
F_{5i} = (c_{13} k_{1i} - e_{31} k_{2i}) s_i^2 - \frac{c_{11}}{2}, \qquad \widetilde{F}_{3i} = \tilde{c}_{13} \tilde{k}_i \tilde{s}_i^2 - \frac{\tilde{c}_{11}}{2}.
$$

Appendix B

The $L(\alpha, \beta)$ in Eq. (40) is as follows:

$$
\begin{aligned}
L(\alpha,\beta) = \frac{4}{\pi^2 m_0} \sum_{i=1}^{3}\sum_{j=1}^{3} M_i \varepsilon_{jkl} \frac{F_{1j}}{s_i s_j} \int_0^\infty \frac{1}{\triangle(\xi)} \sinh\left(\frac{\xi\alpha}{s_j}\right) \sinh\left(\frac{\xi\beta}{s_i}\right) \Bigg\{ & \frac{F_{4i}}{s_i} h_{2k}(\xi) h_{3l}(\xi) K_1\left(\frac{b\xi}{s_i}\right)\\
& + \frac{h_{4i}(\xi)}{s_i} h_{3k}(\xi) h_{1l}(\xi) K_1\left(\frac{b\xi}{s_i}\right) + \frac{h_{5i}(\xi)}{s_i} h_{1k}(\xi) h_{2l}(\xi) K_1\left(\frac{b\xi}{s_i}\right) + \frac{h_{6i}}{s_i} h_{3k}(\xi) h_{1l}(\xi) K_0\left(\frac{b\xi}{s_i}\right)\\
& + \frac{h_{7i}}{s_i^2} h_{2k}(\xi) h_{1l}(\xi) K_0\left(\frac{b\xi}{s_i}\right) + \frac{h_{8i}}{s_i^2} h_{1k}(\xi) h_{2l}(\xi) K_2\left(\frac{b\xi}{s_i}\right) \Bigg\} \mathrm{d}\xi,
\end{aligned}
\tag{B.1}
$$

where

$$
\varepsilon_{jkl} = \begin{cases} 1, & \text{for an even permutation of } 123,\\ -1, & \text{for an odd permutation of } 123,\\ 0, & \text{otherwise,} \end{cases} \qquad (k, l = 1, 2, 3).
$$

References

Chen, W.Q., Shioya, T., 1999. Fundamental solution for a penny-shaped crack in a piezoelectric medium. J. Mech. Phys. Solids 47, 1459–1475.

Chen, W.Q., Shioya, T., 2000. Complete and exact solutions of a penny-shaped crack in a piezoelectric solid: antisymmetric shear loadings. Int. J. Solids Struct. 37, 2603–2619.

Dunn, M., 1994. The effects of crack face boundary conditions on the fracture mechanics of piezoelectric solids. Eng. Fract. Mech. 48, 25–39.

Fabrikant, V.I., 1989. Applications of Potential Theory in Mechanics: A Selection of New Results. Kluwer Academic Publishers, The Netherlands.

Gao, C.F., Fan, W.X., 1999a. Exact solutions for the plane problem in piezoelectric materials with an elliptic or a crack. Int. J. Solids Struct. 36, 2527–2540.

Gao, C.F., Fan, W.X., 1999b. A general solution for the plane problem in piezoelectric media with collinear cracks. Int. J. Eng. Sci. 37, 347–363.

Jackson, J.D., 1976. Classical Electrodynamics. John Wiley, New York.

Kogan, L., Hui, C.Y., 1996. Stress and induction field of a spheroidal inclusion of a penny-shaped crack in a transversely isotropic piezoelectric material. Int. J. Solids Struct. 33, 2719–2737.

McMeeking, R.M., 1989. Electrostrictive stresses near crack-like flaws. J. Appl. Math. Phys. 40, 615–627.

Pak, Y.E., 1990. Crack extension force in a piezoelectric material. ASME Trans. J. Appl. Mech. 57, 647–653.

Park, S.B., Sun, C.T., 1995a. Effect of electric field on fracture of piezoelectric ceramic. Int. J. Fract. 70, 203–216.

Park, S.B., Sun, C.T., 1995b. Fracture criteria for piezoelectric ceramics. J. Am. Ceram. Soc. 78, 1475–1480.

Satapathy, P.K., Parhi, H., 1979. A Transversely isotropic composite with a penny-shaped crack. Acta Mech. 32, 275–285.

Shindo, Y., Tanaka, K., Narita, F., 1997. Singular stress and electric fields of a piezoelectric ceramic strip with a finite crack under longitudinal shear. Acta Mech. 120, 31–45.

Shindo, Y., Horiguchi, K., Murakami, H., Narita, F., 2001. Single-edge precracked beam test and electric fracture mechanics analysis for piezoelectric ceramics. In: Proc. SPIE—Int. Soc. Opt. Eng. Smart Structures and Devices, Melbourne, pp. 311–320.

Sih, G.C., Chen, E.P., 1981. Cracks in Composite Materials, Mechanics of Fracture 6. Martinus Nijhoff Publishers, The Netherlands.

Sosa, H., 1991. Plane problems in piezoelectric media with defects. Int. J. Solids Struct. 28, 491–505.

Sosa, H., Khutoryansky, N., 1996. New developments concerning piezoelectric materials with defects. Int. J. Solids Struct. 33, 3399–3414.

Wang, B., 1992. Three-dimensional analysis of a flat elliptical crack in a piezoelectric material. Int. J. Eng. Sci. 30, 781–791.

Wang, Z.K., Huang, S.H., 1995. Fields near elliptical crack tip in piezoelectric ceramics. Eng. Fract. Mech. 51, 447–456.

Wang, Z.K., Zheng, B.L., 1995. The general solution of three-dimensional problems in piezoelectric media. Int. J. Solids Struct. 32, 105–115.

Yang, J.H., Lee, K.Y., 2001. Penny shaped crack in three-dimensional piezoelectric strip under in-plane normal loadings. Acta Mech. 148, 187–197.

Zhang, T.Y., Hack, J.E., 1992. Mode-III cracks in piezoelectric materials. J. Appl. Phys. 71, 5865–5870.

Zhang, T.Y., Tong, P., 1996. Fracture mechanics for a mode III crack in a piezoelectric material. Int. J. Solids Struct. 33, 343–359.

Zhao, M.H., Shen, Y.P., Liu, Y.J., Liu, G.N., 1997a. Isolated crack in three-dimensional piezoelectric solid: Part I—Solution by Hankel transform. Theor. Appl. Fract. Mech. 26, 129–139.

Zhao, M.H., Shen, Y.P., Liu, Y.J., Liu, G.N., 1997b. Isolated crack in three-dimensional piezoelectric solid: Part II—Stress intensity factors for circular crack. Theor. Appl. Fract. Mech. 26, 141–149.